4ICEGE Thessaloniki-GREECE 2007

4th International Conference on
Earthquake Geotechnical Engineering
June 25-28, 2007
Paper No. 1499

SPATIAL COHERENCY OF GROUND MOTIONS FOR EMBEDDED STRUCTURES

Melanie WALLING[1], & Norman ABRAHAMSON[2]

ABSTRACT

Ground motion recordings of earthquakes from three 3-D dense arrays, (Chiba, Japan; EPRI Parkfield, California; and EPRI LSST, Taiwan) were used to evaluate the depth dependence of the spatial variation of the ground motion for application for embedded structures. Using these data, the differences between the coherency of the ground motions at surface and at depth are evaluated. The dimensions of these three arrays, allow coherency estimates to be made for station separations of 10 m to 50 m at embedment depths of 10 m to 20 m. The difference between the surface coherency and the coherency at depth are computed for each array separately and also for the combined data. For frequencies up to 20Hz, the average coherency at depths between 10 m – 20 m is greater then at the surface for separation distance bins 0 – 10 m, 10 – 15 m, 15 – 25 m, 25 – 30 m, and 30 – 45 m, by a scale factor of 1.78, 1.66, 1.53 and 1.14 lagged coherency units, respectively. Above 20 Hz, the signal to noise ratio is not adequate to allow estimation of the coherency. These comparisons show that the use of surface coherence for embedded structures will overestimate the potential reduction of the translational response in the high frequency range for separation distances less than 45m.

Keywords: spatial coherency, embedded structures, three-dimensional arrays

INTRODUCTION

The spatial variations of earthquake ground motion over short dimensions of large foundations tend to reduce the high frequency translational response of structures with rigid foundations, while increasing the rocking and torsion responses. This reduction in the high frequency response can be important for seismic response of nuclear power plants in stable continental regions which tend to have increased high frequencies. The spatial variation of ground motions is typically parameterized by empirical coherency functions. Most of the arrays on which the empirical coherency functions are based are surface arrays, but in many applications of the models, the foundations are embedded. In current practice, the surface coherency functions have been assumed to be applicable to both non-embedded and embedded foundations. Here we have used data that include both surface and downhole stations to evaluate this assumption.

DATA

Three-dimensional arrays were not considered here if there was only a single vertical array in the configuration. Multiple stations on a plane at depth are needed to evaluate the coherency at depth, because it is the coherency between the stations located at the same elevation that is used and not the stations that share the same location but are offset in depth relative to the other. Ground motions from 3 dense three-dimensional arrays are used to evaluate the coherency at depth: the Chiba array (Japan), the EPRI LSST array (Taiwan), and the EPRI Parkfield (California).

1. PH.D Candidate, Dept. of Civil and Environ. Engineering, Univ. of California, Berkley, CA mwalling@berkeley.edu
2. Pacific Gas & Electric Company, 245 Market Street, San Francisco, CA, naa2@pge.com

EPRI/Taipower LSST Array
The EPRI LSST array is located in northeastern Taiwan. EPRI and Taipower installed the array in 1985 as part of a joint program. The array consists of free-field surface, free-field downhole, and structure instruments. The surface array consists of 15 three-component force balanced accelerometers. The stations are configured in a Y-shaped array with 85 m radius. The downhole instruments are located on Arm 1 of the array, beneath locations DHA and DHB, at four depths, 6 m, 11 m, 17 m, 47 m. Only the free-field surface stations FA1-1 and FA1-5, and the free-field downhole DHA and DHB stations at depths 6 m and 11 m from this array were used for this study.

Anderson and Tang, (1987) conducted extensive in situ and laboratory studies to define the soil statigraphy and geotechnical properties beneath the LSST array. Samples were taken from the 12 holes that were drilled to depths of 30 m to 150 m. From cross-hole and u-hole seismic tests Anderson and Tang (1987) determined that the S-wave velocities are 100 m/s near the surface and increases to 250 m/s at 18 m depth and remains 250 m/s to a depth of 50 m.

EPRI Parkfield Array
EPRI installed a densely spaced strong motion array at Stone Corral, approximately 15 km southeast of Parkfield. The array is located in fairly flat topography, 7 km east of the San Andreas Fault along the rupture zone of the 1966 Parkfield earthquake. The array was in operation from November 1987 to 1996. Array was not operating during the 2004 Parkfield earthquake.

The array consists of 21 three-component force-balanced accelerometers connected to a central recording facility on site. There are 13 surface and 8 downhole elements distributed to a 90 m depth. The surface stations are configured in a Y-shaped array with a 120 m radius. Four downhole elements are also configured in a Y-shaped array, beneath stations W2, SE2, NE2, and G0, at a depth of 15 m.

The site array is located in a complex tectonic block on the northeast side of the San Andreas Fault. In this area, the deep basement is composed of previously sheared Franciscan and related ultramafic rocks of Mesozoic age. The basement rocks are overlain by about 5000 m of Tertiary and Cretaceous marine sedimentary rocks. The basement and overlying meta-sedimentary rocks have been progressively transposed into a series of NW-SE trending enchelon and faulted folds, probably in response to the right-lateral shear associated with the San Andreas Fault system.

The central portion of the seismic array is located on an old (>10,000 years) alluvial deposit which is up to about 6 m thick. The bedrock underlying and surrounding the array is predominantly sandstone of the Miocene Temblor Formation (Diblee, 1971). The small area of the mudstone and siltstone is also mapped at the surface in the northwestern portion of the array. The array is located on the eastern limb of a steep, NW plunging, N40W trending asymmetric syncline. At the array center, the Temblor formation extends from 6 m depth to below 90 m, with a bedding plane dip of 70 degrees.

Chiba Array
The Chiba array is located at the Chiba experiment station approximately 30 km east of Tokyo. The Chiba array consists of 15 three-component near surface accelerometers, an approximate 300 m x 400 m footprint. The near-surface stations are buried at a depth of 1 m. Within this array, there is a very dense sub-array that contains 9 stations in an approximate footprint of 30 m x 30m. There are also 29 three-component downhole accelerometers at depths ranging from 5 to 40 m.

The array site has uniform soil; the soil profile consists of about 3 – 5 km of loam over about 5 m of sandy clay and clayey sand. There is more than 30 m of fine sands below the clayey sands. The shear wave velocities of these layers are approximately 140 m/s, 320 m/s, and 320 – 420 m/s, respectively. A complete description of the array is given by Katayama et al. (1990).

An example recording from each array is shown in Figure 1. The earthquakes for the 3 arrays, the depths, the number of station pairs and the separation distances used for this analysis are summarized in Table 1, below.

Table 1 Data used to evaluate the coherency depth effect

Array	Eqk Number	Date	Depths	Total Station Pairs	Separation Distance (m)
1	3	11/8/89	11	2	45,45
1	4	1/17/90	11	2	45,45
1	5	3/30/90	11	2	45,45
1	8	5/21/90	11	2	45,45
1	10	7/17/90	11	2	45,45
1	12	7/31/90	11	2	45,45
1	14	7/31/90	11	2	45,45
1	16	11/15/90	11	2	45,45
1	17	11/15/90	11	2	45,45
2	1	10/24/92	15	3	45,45,45
2	2	5/26/93	15	3	25,25,45
3	8307	2/28/87	10,20	10	15,15,15,15,21,21,21,21,30,30
3	8420	12/18/88	10,20	10	15,15,15,15,21,21,21,21,30,30
3	8510	6/9/89	10,20	10	15,15,15,15,21,21,21,21,30,30
3	8519	10/5/89	10,20	10	15,15,15,15,21,21,21,21,30,30
3	8525	11/17/89	10,20	10	15,15,15,15,21,21,21,21,30,30
3	8722	12/18/91	10,20	10	15,15,15,15,21,21,21,21,30,30
3	8806	1/17/92	10,20	10	15,15,15,15,21,21,21,21,30,30
3	8816	3/19/92	10,20	10	15,15,15,15,21,21,21,21,30,30
3	8901	2/20/93	10,20	10	15,15,15,15,21,21,21,21,30,30

1. LSST; 2. PARKFIELD; 3. CHIBA

METHODOLOGY

The spatial variation of the Fourier phase of strong ground motion can be quantified by various parameters such as the correlation or coherency. The correlation is a time domain measure while the coherency is a frequency domain measure. In practice, it is common to characterize the spatial variation of the phase using the coherency.

In this study, the coherency analysis procedure used by Abrahamson (1992) for the EPRI Lotung array is followed. The estimation of coherency is briefly discussed below. A more detailed discussion is given by Abrahamson (1992).

Let $u_j(\omega)$ be the Fourier transform of the tapered time series uj(t), then

$$u_j(\omega) = \sum_{k=1}^{T} v(t_k) \exp\{-i\omega t_k\} \tag{1}$$

where $v(t_k)$ is the data taper, T is the number of time samples, t_k is the time of the k^{th} samples, and ω is the frequency. The smoothed cross-spectrum is given by

$$S_{jk}(\omega) = \sum_{m=-M}^{M} a_m u_j(\omega_m) \bar{u}_k(\omega_m) \tag{2}$$

where 2M+1 is the number of discrete frequencies smoothed, $\omega_m = \omega + 2\pi m/T$, a_m are the weights used in the frequency smoothing, and the overbar indicates the complex conjugate. The coherency, $\gamma_{ij}(\omega)$, is given by

$$\gamma_{ij}(\omega) = \frac{S_{ij}(\omega)}{S_{ii}(\omega)S_{jj}(\omega)} \tag{3}$$

where $S_{ij}(\omega)$ is the smoothed cross-spectrum for stations i and j. As shown in Eq. 3 the coherency is a complex number. Typically the absolute value of coherency, $|\gamma_{ij}(\omega)|$, called the lagged coherency is used as the primary description of the spatial variation. The coherency is heteroscadastic, therefore a homoscadasitc transformation is needed to make it a consistent estimator. Enochson and Goodman, (1968) determined a $\tanh^{-1}$ transformation does this. For this paper, we analyze the transformed $|\gamma(\omega)|$ and refer to it as the transformed lagged coherency. Figure 2 shows that the range of the coherency standard deviation is approximately constant across frequencies.

For this analysis the transformed lagged coherencies of the two horizontal components were averaged and the ratio between depth and surface were computed. Averaging both horizontal components removed the effect of accelerometer orientation with respect to the recorded earthquake. Only data with separation distances less than 50 m and frequencies less than 25Hz were evaluated.

RESULTS

The depth effect of the coherence is analyzed using three different weighting schemes. The first scheme gave equal weighting to each station pair; the second scheme gave equal weighting to each earthquake; and the third scheme gave equal weighting to each array. For all applicable frequencies, the average mean, standard deviation, median, and the number of data points used for the first scheme are found below in Table 2. The mean, standard deviation, and the median of the second and third scheme are within 10% of these values.

Table 2. Mean, standard deviation, and median of the Ratio (embedded atanh |γ| / free-field atanh |γ|) and number, N, data points used with equal weight to each station.

Distance Bin	Mean	Std.Dev	Median	N
0 - 10	1.78	1.23	1.426	1999
10 - 15	1.66	1.71	1.375	1800
15 - 25	1.6	1.07	1.309	1824
25 - 30	1.53	0.96	1.29	900
30-45	1.14	0.65	1.03	272

The coherency depth effect for each station pair versus frequency and separation distance is shown for separation distance bins 0 – 10 m, 10 - 15 m, 15 – 25 m, 25 – 30 m, and 30 – 45 m in Figure 3. Only ratios up to 7 are shown in these figures, however ratios up to 14 were computed. These high ratios occurred at frequencies less than 5 hz. This occurred because the atanh transformation becomes exponential for values approaching 1.0. At frequencies less than 5 Hz small changes in lagged coherency can translate into large ratios when comparing transformed lagged coherency.

CONCLUSION

The spatial variability of the ground motions at the surface is greater than the embedded ground motions for separation distances less than 45 m and frequencies less than 20 Hz. The significance of the coherency depth effect is dependent on the frequency and the separation distance as seen in Figure

3. The longer periods of the surface motion will approximate the embedded motion for separation distances less than 10 m, will underestimate the coherency for separation distances that are approximately between 10 m and 40 m, and becomes insignificant at separation distances of 45 m. The short periods of surface motion will underestimate the coherency of the embedded motions for separation distances less than 40 m, becoming less significant as the separation distance increases to 40m and becomes insignificant at separation distances of 45 m.

From Figure 3 separation distances less than 45 m, we conclude that a simple constant factor or scaling factor applied to the surface coherency model is needed to approximate the embedded coherency for separation distances between 10 m and 45 m; however from Figure 3 plot of the separation distance equal to 45 m, we conclude that for these distances the surface coherency model is similar to the embedded coherency for frequencies less than 20 Hz. For separation distances less than 10 m, a more complicated correction is needed that will approximate the depth effect at short periods, but which will reduce to zero or scale to 1.0 at long periods.

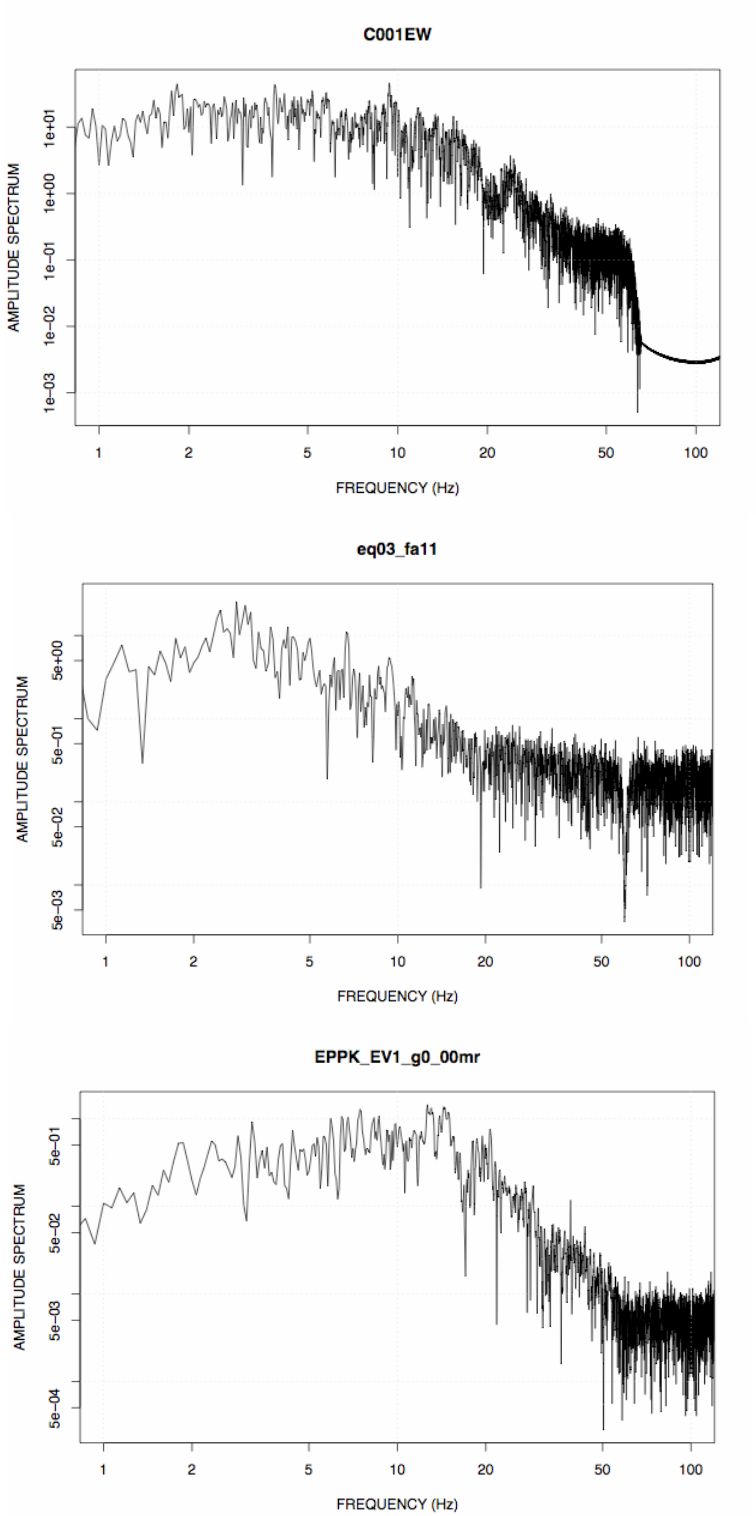

Figure 1. An example of the dynamic range of the three Fourier amplitude spectrums from the windowed acceleration recordings: 8307_C001.acc, Chiba array (top); eq03_fa11.acc, LSST array (middle); EPPK_EV1_g0_00mr.acc, Parkfield array (bottom).

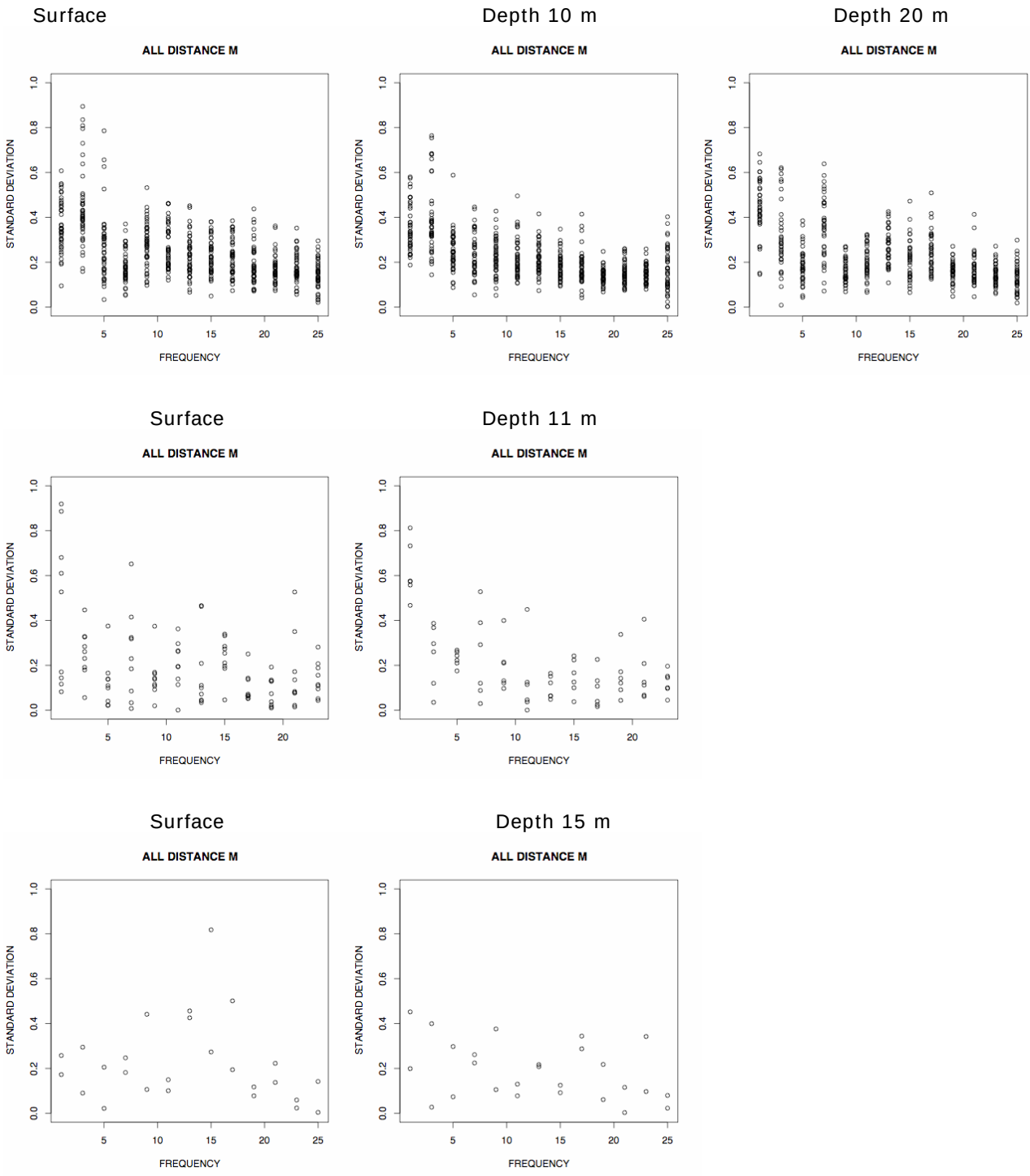

Figure 2. Standard deviation computed for each station of array, Chiba (top), LSST (top), and Parkfield (bottom) and plotted as a function of frequency for the surface recordings and the embedded recordings. The standard deviation is relatively constant with depth and with frequency.

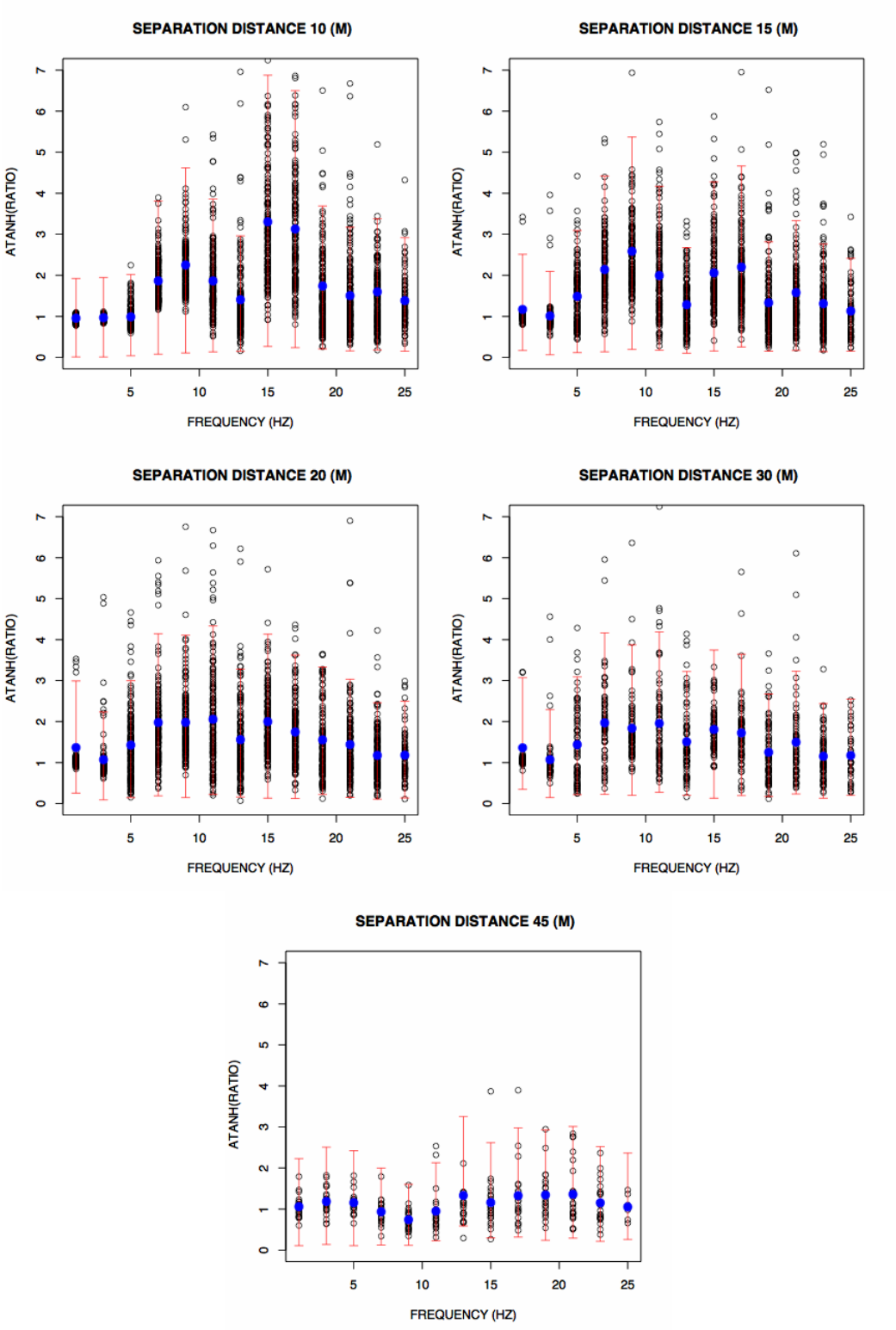

Figure 3. The ratio(embedded transformed lagged coherency / free-field transformed lagged coherency) for each stations of array Chiba, LSST, and Parkfield are shown as black circles plotted as a function of 2 Hz frequency bins for five separation distances bins: 10 m ,15 m, 20 m, 30 m, 45 m. Blue circles are the mean of the ratio computed for each frequency bin with the 95% confidence limits shown in red.

REFERENCES

Abrahamson, N.A. (1992). Spatial variation of earthquake ground motion for application to soil-structure interaction, EPRI Report 2978-1.

Anderson, D.G. and H.T.Tang (1987). Summary of soil characterization program for the Lotung Large-scale seismic experiment, *Proc:Workshopon Lotung Large Scale Seismic Experiment*, EPRI, Palo Alto, CA, December 1987.

Diblee, T.W., Jr., (1971), Geologic maps of 17 15 minute quadrangles along the San Andreas fault in the vicinity of King City, Coalinga, Panoche Valley and Paso Robles, with index map: U.S. Geological Survey Open-File Report 71-87, scale 1:62,500.

Enochson, L.D. and N.R. Goodman (1965) Gaussain approximationto the distribution of sample coherence, Tech Report, AFFDL-TR-65-57, Wright-Patterson Air Force Base.

Katayama, T., F. Yamazaki,F., S.Nagata, L. Lu, and T.Turker (1990). Development of strong motion database of the Chiba seismometer array, Earthquake Disaster Mitigation Engineering, Institute of Industrial Science, University of Tokyo, Report No. 90-1 (14).